

## Introducing QuantConn

**Citation for published version (APA):**

Newlin, N., Schilling, K., Koudoro, S., Chandio, B. Q., Kanakaraj, P., Moyer, D., Kelly, C. E., Genc, S., Yang, J. Y.-M., Wu, Y., Adluru, N., Nath, V., Pathak, S., Schneider, W., Gade, A., Consagra, W., Rathi, Y., Hendriks, T., Vilanova, A., ... Landman, B. (2025). Introducing QuantConn: Overcoming Challenging Diffusion Acquisitions with Harmonization. In M. Chamberland, T. Hendriks, M. Karaman, R. Mito, N. Newlin, S. Shailja, & E. Thompson (Eds.), *Computational Diffusion MRI: 15th International Workshop, CDMRI 2024, Held in Conjunction with MICCAI 2024, Marrakesh, Morocco, October 6, 2024, Proceedings* (pp. 164-174). (Lecture Notes in Computer Science (LNCS); Vol. 15171). Springer. [https://doi.org/10.1007/978-3-031-86920-4\\_15](https://doi.org/10.1007/978-3-031-86920-4_15)

**Document license:**

TAVERNE

**DOI:**

[10.1007/978-3-031-86920-4\\_15](https://doi.org/10.1007/978-3-031-86920-4_15)

**Document status and date:**

Published: 18/04/2025

**Document Version:**

Publisher's PDF, also known as Version of Record (includes final page, issue and volume numbers)

**Please check the document version of this publication:**

- A submitted manuscript is the version of the article upon submission and before peer-review. There can be important differences between the submitted version and the official published version of record. People interested in the research are advised to contact the author for the final version of the publication, or visit the DOI to the publisher's website.
- The final author version and the galley proof are versions of the publication after peer review.
- The final published version features the final layout of the paper including the volume, issue and page numbers.

[Link to publication](#)

**General rights**

Copyright and moral rights for the publications made accessible in the public portal are retained by the authors and/or other copyright owners and it is a condition of accessing publications that users recognise and abide by the legal requirements associated with these rights.

- Users may download and print one copy of any publication from the public portal for the purpose of private study or research.
- You may not further distribute the material or use it for any profit-making activity or commercial gain
- You may freely distribute the URL identifying the publication in the public portal.

If the publication is distributed under the terms of Article 25fa of the Dutch Copyright Act, indicated by the "Taverne" license above, please follow below link for the End User Agreement:

[www.tue.nl/taverne](http://www.tue.nl/taverne)

**Take down policy**

If you believe that this document breaches copyright please contact us at:

[openaccess@tue.nl](mailto:openaccess@tue.nl)

providing details and we will investigate your claim.



# Introducing QuantConn: Overcoming Challenging Diffusion Acquisitions with Harmonization

Nancy Newlin<sup>1</sup>✉, Kurt Schilling<sup>2</sup>, Serge Koudoro<sup>3</sup>, Bramsh Qamar Chandio<sup>4</sup>,  
Praitayini Kanakaraj<sup>1</sup>, Daniel Moyer<sup>1</sup>, Claire E. Kelly<sup>5,6,7</sup>, Sila Genc<sup>8,9</sup>,  
Joseph Yuan-Mou Yang<sup>5,8,9,10</sup>, Ye Wu<sup>11</sup>, Nagesh Adluru<sup>12</sup>, Vishwesh Nath<sup>13</sup>,  
Sudhir Pathak<sup>14</sup>, Walter Schneider<sup>14</sup>, Anurag Gade<sup>15</sup>, William Consagra<sup>16</sup>,  
Yogesh Rathi<sup>16</sup>, Tom Hendriks<sup>17</sup>, Anna Vilanova<sup>17</sup>, Maxime Chamberland<sup>17</sup>,  
Tomasz Pieciak<sup>18,19</sup>, Dominika Ciupek<sup>19</sup>, Antonio Tristán Vega<sup>18</sup>,  
Santiago Aja-Fernández<sup>18</sup>, Maciej Malawski<sup>19</sup>, Gani Ouedraogo<sup>20</sup>,  
Julia Machnio<sup>19</sup>, Paul M. Thompson<sup>4</sup>, Neda Jahanshad<sup>4</sup>,  
Eleftherios Garyfallidis<sup>3</sup>, and Bennett Landman<sup>21,22</sup>

<sup>1</sup> Department of Computer Science, Vanderbilt University, Nashville, TN, USA  
[nancy.r.newlin@vanderbilt.edu](mailto:nancy.r.newlin@vanderbilt.edu)

<sup>2</sup> Department of Radiology and Radiological Sciences, Vanderbilt University Medical Center, Nashville, USA

<sup>3</sup> Indiana University Bloomington, Bloomington, IN, USA

<sup>4</sup> Mark and Mary Stevens Neuroimaging and Informatics Institute, Keck School of Medicine of USC, Los Angeles, CA, USA

<sup>5</sup> Developmental Imaging, Murdoch Children' Research Institute, Melbourne, Australia

<sup>6</sup> Victorian Infant Brain Study (ViBeS), Murdoch Children's Research Institute, Melbourne, Australia

<sup>7</sup> Turner Institute for Brain and Mental Health, School of Psychological Sciences, Monash University, Melbourne, Australia

<sup>8</sup> Neuroscience Advanced Clinical Imaging Service (NACIS), Department of Neurosurgery, Royal Children's Hospital, Melbourne, Australia

<sup>9</sup> Neuroscience Research, Murdoch Children's Research Institute, Melbourne, Australia

<sup>10</sup> Department of Paediatrics, University of Melbourne, Melbourne, Australia

<sup>11</sup> School of Computer Science and Technology, Nanjing University of Science and Technology, Nanjing, China

<sup>12</sup> Waisman Center, Department of Radiology, University of Wisconsin, Madison, USA

<sup>13</sup> NVIDIA, Santa Clara, USA

<sup>14</sup> Learning Research and Development Center, University of Pittsburgh, Pittsburgh, USA

<sup>15</sup> Brigham and Women's Hospital, Boston, USA

<sup>16</sup> Brigham and Women's Hospital, Harvard Medical School, Boston, USA

<sup>17</sup> Department of Computer Science and Mathematics, Eindhoven University of Technology, Eindhoven, The Netherlands

<sup>18</sup> LPI, ETSI Telecomunicación, Universidad de Valladolid, Castilla y León, Spain

<sup>19</sup> Sano Centre for Computational Medicine, 30-054 Kraków, Poland

<sup>20</sup> Aix-Marseille Université, Marseille, France

<sup>21</sup> Vanderbilt University Institute of Imaging Science, Vanderbilt University,  
Nashville, TN, USA

<sup>22</sup> Department of Electrical and Computer Engineering, Vanderbilt University,  
Nashville, TN, USA

**Abstract.** White matter alterations are increasingly implicated in neurological diseases and their progression. Diffusion-weighted magnetic resonance imaging (DW-MRI) has been included in many international-scale studies to identify alterations in white matter microstructure and connectivity. Yet, quantitative investigation of DW-MRI data is hindered by a lack of consistency due to variations in acquisition protocols, sites, and scanners. Specifically, there is a need to harmonize the preprocessing of DW-MRI datasets to ensure that compatible and reproducible quantitative metrics are derived from each site, including (1) bundle-wise microstructure measures, (2) features of white matter fiber bundles, and (3) connectomics measures. In the MICCAI CDMRI 2023 QuantConn challenge, participants are provided raw data from the same individuals taken with two different acquisition protocols on a single 4 tesla scanner in the same scanning session and asked to preprocess the data in order to minimize acquisition differences while retaining biological variation. Here, we outline the testing framework, provide baseline pre-harmonized results, and discuss the learning implications of this challenge.

**Keywords:** Diffusion MRI · harmonization · macrostructure · microstructure · tractography · connectome · image processing

## 1 Introduction

Diffusion-weighted magnetic resonance imaging (DW-MRI) is a non-invasive imaging modality that enables in-vivo modeling of white matter microstructure and facilitates structural brain connectivity mapping. DW-MRI has been included in many international-scale studies focused on white matter biomarkers in development, disease, and disorders. Yet, multi-site investigation of DW-MRI data is hindered by a lack of consistency due to variations in acquisition protocols, scanner settings, and manufacturers [17]. Substantial progress has been made with calibration and harmonization to reduce inter-subject variance and improve the interpretability of computed measures. However, the fundamental challenge remains that the clinical application of DW-MRI (as currently implemented) is confounded by inter-scanner and inter-site effects. Here, we introduce the QuantConn challenge - an international community challenge which aims to harmonize differences in diffusion acquisitions.

This challenge builds off the successful SuperMUDI [15] and MUSHAC [13] challenges. In SuperMUDI, participants were tasked with super-resolving data ( $N=5$  volunteers) that have high in-plane resolution but thick (axial) slices in order to match an isotropically acquired dataset. In the MUSHAC challenge, participants were given datasets ( $N=15$  volunteers) that were acquired on two different scanners, with two different acquisitions on each, and tasked with minimizing cross-scanner and cross-protocol differences in voxel-wise indices. Here, we provide 103 pairs of datasets of the same subjects, scanned with very different acquisition protocols - and challenge participants to minimize differences in the data in order to minimize differences in microstructure, tractography bundle analysis, and connectomics measures. The key innovations of the QuantConn challenge are (1) we assess bundles and tractography in the context of harmonization for the first time, (2) we assess connectomics in the context of harmonization for the first time, and (3) we have 10x additional subjects over MUSHAC and 100x over SuperMUDI. Additionally, the data that form the basis of this challenge represent a difficult clinical scenario for harmonization and are part of a much larger twins study, which could provide rich context for continuing validation and extension of this challenge’s findings.

In the following, we introduce the challenge, describe the data and evaluation framework, and present baseline measures against which challenge submissions will be compared against. We end with a discussion on what we aim to investigate, and hope to learn from this community effort.

## 1.1 The Challenge

Participants are challenged to bridge acquisition disparities in scan-rescan DW-MRI data - using potentially preprocessing, super-resolution, and/or harmonization techniques. They are provided with a T1-weighted MRI and two DW-MRI scans for a cohort of 78 training and 25 testing patients. The core differences between the two acquisitions are (1) spatial resolution ( $1.8 \times 1.8 \times 5 \text{ mm}^3$  vs.  $1.8 \times 1.8 \times 2 \text{ mm}^3$ ) and (2) number of directions collected (27 vs. 94). These differences bias and confound three major groups of diffusion analysis: bundle microstructure, bundle macrostructure, and complex network measures (Fig. 1) [11, 17, 20, 21]. A successful challenge algorithm will minimize protocol differences in all three analyses.

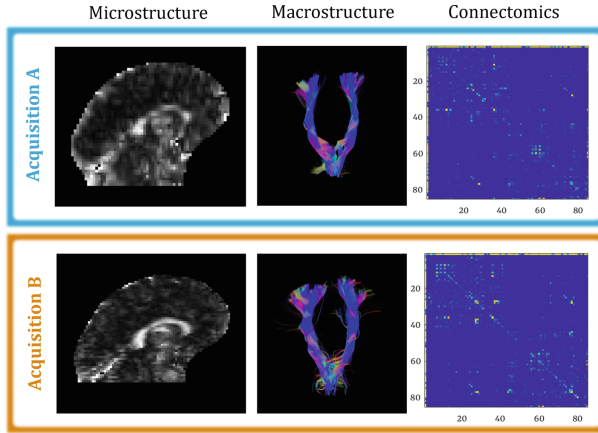


**Fig. 1.** Acquisition differences affect microstructure measurements (FA map, left), macrostructure reconstructions (corticospinal tract shape, middle), and connectomics (whole brain connectome, right).

## 2 Data

The data that form the basis of this challenge represent a difficult clinical scenario for harmonization and are a subset of the Queensland Twin Imaging study [19]. The DW dataset consists of 25 matched testing and 78 training subjects scanned twice with two different acquisition protocols (Fig. 2). Testing and Training data used in this challenge are publicly available at [shared Box](#). Each subject has an anatomical 3D whole-brain T1-weighted image. The data subset is comprised of 45% females, ages  $25.3 \pm 1.8$  years. No subjects reported a history of significant head injury, neurological or psychiatric illness, or substance abuse or dependence, and no subjects had a first-degree relative with a psychiatric disorder. All subjects were right-handed as determined using 12 items from Annett’s Handedness Questionnaire [2]. Scanning was performed at the QIMR Berghofer Medical Research Institute on a 4 tesla Siemens Bruker Medspec scanner [19].

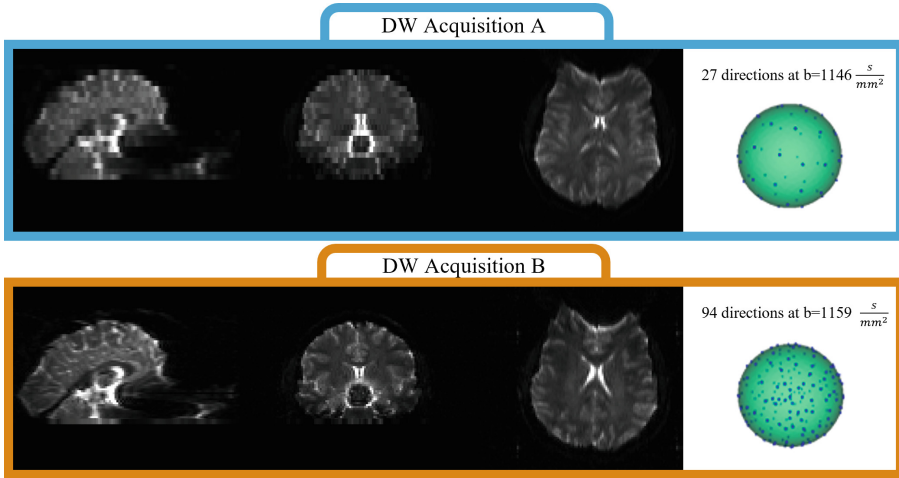


**Fig. 2.** Each subject was scanned using two protocols with different resolutions (left) and gradient directions (right). Image resolution and quality differences are apparent in visualizations of  $b_0$ -images ( $b = 0 \text{ s/mm}^2$ ).

## 2.1 Acquisition A

Acquisition A DW images were acquired using single-shot echo-planar imaging with a twice-refocused spin echo sequence. Imaging parameters were repetition/echo times of 6090/91.7 ms, field of view of 23 cm, and  $128 \times 128$  acquisition matrix. Each 3D volume consisted of 21 axial slices 5 mm thick with a 0.5 mm gap and  $1.8 \times 1.8 \text{ mm}^2$  in-plane resolution, total time = 3 min. Thirty images were acquired per subject: three with no diffusion sensitization ( $b = 0 \text{ s/mm}^2$ ) and 27 DW images ( $b = 1146 \text{ s/mm}^2$ ) with gradient directions uniformly distributed on the hemisphere.

## 2.2 Acquisition B

Acquisition B DW images were acquired using single-shot echo planar imaging (EPI) with a twice-refocused spin echo sequence. Imaging parameters were: 23cm FOV, TR/TE 6090/91.7 ms, with a  $128 \times 128$  acquisition matrix. Each 3D volume consisted of 55 2-mm thick axial slices with no gap and a  $1.79 \times 1.79 \text{ mm}^2$  in-plane resolution with total acquisition time = 14.2 min. 105 images were acquired per subject: 11 with no diffusion sensitization ( $b = 0 \text{ s/mm}^2$ ) and 94 DWI ( $b = 1159 \text{ s/mm}^2$ ) with gradient directions uniformly distributed on the hemisphere.

## 3 Testing Framework

Participants will submit 25 paired DW-MRI from the testing cohort. Submission processing includes: diffusion analysis of tensor fitting, orientation distribution

function (ODF) reconstruction, whole brain tractography, bundle segmentation, tractometry, bundle shape analysis, connectomics, and finally, complex network analysis. Code is available via a [public docker](#). Testing data are 2.9 GB and evaluation takes 9 h on a 64 GB RAM Macbook Pro.

Assessment will be performed to quantify the similarity of (1) bundle-specific microstructure measures, (2) macrostructural features of each pathway, and (3) complex network measures. Table 1 reports the baseline scores for each category.

**Table 1.** Baseline scores for un-harmonized data.

Connectivity score	Microstructural score	Shape similarity score	Shape profile score
0.37	0.19	0.85	6.79

### 3.1 Bundle-Specific Microstructure

Microstructure measures of fractional anisotropy (FA), mean diffusivity (MD), geodesic anisotropy (GA), radial diffusivity (RD), and axial diffusivity (AD) are calculated for each of six pathways as the average DTI measure within each bundle: left/right Arcuate Fasciculus (AF), left/right Optic Radiations (OR), and left/right Corticospinal tract bundles (CST)

Ideally, DTI in these ROIs would be the same across scans for a single patient. However, Fig. 1 shows bundles are not consistent across acquisitions A and B. We use Intra-class Correlation Coefficient (ICC) to quantify reproducibility across acquisitions and bundles. ICC quantifies how well measurements of the same group resemble each other. The QIBA Technical Performance Working Group suggests using ICC to evaluate repeatability. The ICC is interpreted as follows: below 0.5 as “poor”, between 0.50 and 0.75 as “moderate”, between 0.75 and 0.90 as “good”, and above 0.90 as “excellent” [10]. We evaluate the repeatability of diffusion measures for scan-rescan of the same subject, for all 25 subjects in the testing cohort. Baseline results for ICC per bundle, before any preprocessing or harmonization solution has been applied, is reported in Fig. 3. We compute a single microstructural score that is the average ICC across bundles. Successful submissions will increase ICC and have a higher microstructural score than that reported in Table 1.

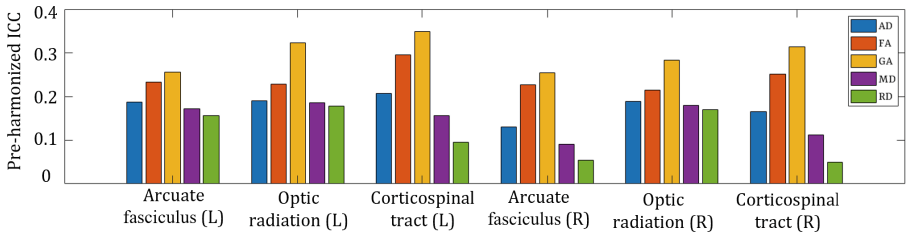


**Fig. 3.** ICC, computed across 25 A/B pairs, of bundle microstructural measures AD, FA, GA, MD, RD for 6 bundles. Successful submissions will improve consistency of microstructural measures and have higher ICC values.

### 3.2 Bundle-Specific Macrostructure

Using the same six bundles above, we use the BU $\text{N}$ dle ANalytics (BUAN) framework to compare the reconstructions created from each acquisitions' DW-MRI [5],[?].

BUAN provides bundle shape similarity scores to assess structural consistency among bundles. Bundle shape similarity is a streamline-based comparison approach that provides a single score between 0 (no match) and 1 (perfect match) between two bundles. Furthermore, we created bundle shape profiles using BundleWarp registration [4]. The bundle shape profile describes shape differences in bundles across the two acquisitions in terms of deformation magnitude generated by BundleWarp registration to match two bundles completely. Lower deformation magnitude implies fewer shape differences in two bundles, and higher deformation magnitude means a high number of deformations and/or transformations are required to align two bundles perfectly, hence having higher shape differences.

Bundle shapes should be consistent across scans of the same patient. Thus, we expect a successful submission will produce DW-MRI that has low bundle shape profiles and high shape similarity scores across acquisitions. The bundle shape profile and shape similarity scores are reported for 25 Test patients in Fig. 4. The final bundle-based score is the average across all 25 patients.

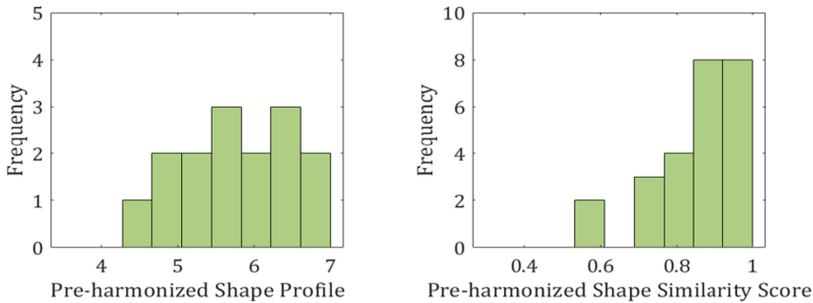


**Fig. 4.** BundleWarp macrostructure comparison measures, bundle shape profiles (left) and bundle shape similarity score (right), computed across acquisitions for all 25 test-set patients. Successful submissions will improve DW-MRI quality such that bundle shape similarities are higher and bundle shape profiles are lower.

### 3.3 Connectome Measures

The last class of metrics that we derive are complex network measures computed on the connectome. To construct a connectome, we first reconstruct ODFs using the Constant Solid Angle (CSA) algorithm at a maximum spherical harmonic order of 6 [1]. Using the ODF and a white matter mask ( $FA > 0.1$ ), we perform whole-brain tractography using the EuDX [7] algorithm. The connectome is the result of segmenting and mapping the whole brain tractogram into brain

regions (nodes) and the streamlines connecting them (edges). For this challenge, tractograms are segmented based on the Desikan-Killiany atlas from FreeSurfer (version 7.2.0) with 87 cortical and subcortical regions [6].

Connectome measures are intended to characterize brain networks in a computationally simple yet meaningful manner [16]. In this challenge, we consider modularity, assortativity, average participation coefficient, density, average node strength, and average clustering coefficient. Modularity is the degree to which the network can be subdivided into clearly delineated subgroups and summarizes the community structure. Assortativity is a correlation coefficient between nodes of opposite ends of a link and reflects the network’s resilience. The participation coefficient is a measurement of the diversity of intermodular connections. Density is the fraction of present connections to total possible connections. Node strength is the sum of weights for edges connected to a given node. The clustering coefficient is the geometric mean associated with a node. We use the *scipy* (version 1.5.0) and *bctpy* (version 0.6.1) implementations of the Brain Connectivity Toolbox measure definitions [16].

A successful submission would produce DW-MRI with consistent complex network measures across acquisitions of the same patient. Figure 5 is a histogram report highlighting the significant baseline differences between acquisitions. We assess reproducibility across complex network measures with ICC. This ICC is the final connectivity score (Table 1).

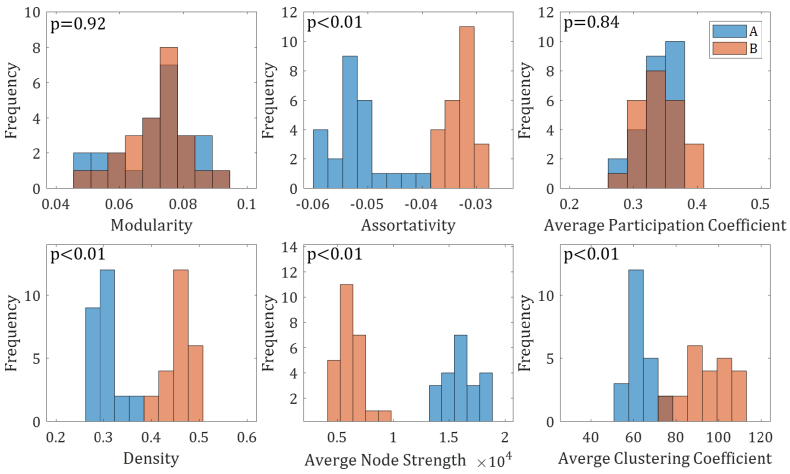


**Fig. 5.** Histogram distributions for connectome measures derived from pre-harmonized A and B DWI acquisitions. t-test p-values for comparing means across the two acquisitions are reported in the top left corner.

## 4 Broader Contributions

Data are increasingly coming from multi-center, multi-site, and multi-acquisition sources, and it is important to utilize these datasets to detect changes in

development [3,9,18], Alzheimer’s disease [12,14], and autism [8]. For this reason, harmonization is particularly important in DW-MRI so that bundles and connectomes are comparable, and we can study features from micro-scale to macro-scale. These features act as potential biomarkers for neurological diseases, and subtle, important changes can be overshadowed by un-harmonized biases.

This challenge gives us insight into the efficacy of diffusion harmonization methods that aim to make one site acquisition like another. Current examples include statistical and image-based methods, which have proven useful so far, but methods are continuously being developed and improved. This study is a benchmark that lets us define method successes and limitations. A successful submission in this challenge is one that overcomes the dramatic differences due to resolution and gradient directions. While this challenge tasks image-based methods of diffusion harmonization, i.e. making the signal from scanners similar, we do not specifically investigate statistical approaches which have become common in literature (ComBat, CovBat, NeuroCombat). As an extension of this challenge and all submissions, we plan to investigate the fidelity and robustness of statistical feature based harmonization methods. For example, we are not aware of these approaches being applied to features of bundles.

Beyond simple harmonization, this challenge also acts as a super-resolution task. The task of super resolution is simply to perform image processing that results in an image with information captured at a higher resolution than it was acquired at. This method is important in tractography to make data isotropic, and is more critical as we try to investigate smaller structures in the brain. A successful submission in this challenge will necessitate super-resolving the low resolution dataset to generate a higher, isotropic resolution dataset that closely matches signal actually acquired at a higher spatial resolution.

Finally, preprocessing is necessary to remove effects and biases and improve SNR. For example, preprocessing mitigates motion, susceptibility and eddy current distortions - a necessary step for robust, reproducible measurements. Because these data have different acquisitions and, therefore, different artifacts and distortions, this is a study on preprocessing techniques that minimize differences due to imaging artifacts.

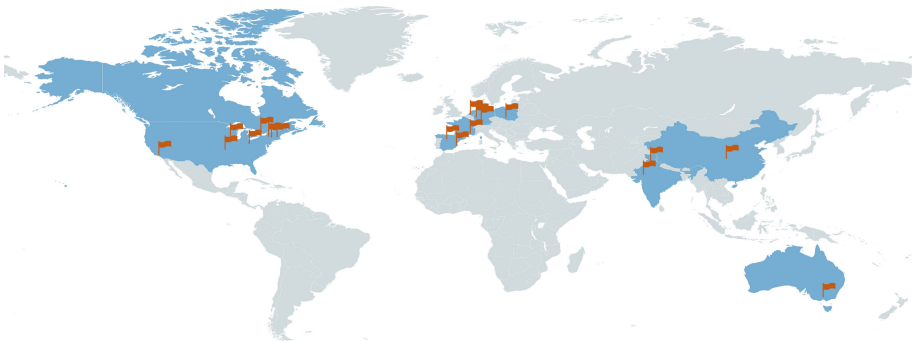


**Fig. 6.** Twenty teams from across the world have registered to participate in the Quant-Conn challenge. This map visualization was made with mapchart.com.

We expect participants (Fig. 6) to submit a range of methods such as explicit signal harmonization, resolution adjustments, and machine learning solutions.

**Acknowledgements.** The Queensland Twin Imaging study data collection was funded by National Institute of Child Health and Human Development (R01 HD050735), and National Health and Medical Research Council (496682, 1009064).

This work was also supported in part by NIH grants R01EB017230, NIDDK K01EB032898, R01NS123378, P50HD105353, RF1AG057892 (FiberNET project grant), R01 MH134004 and R01MH119222 (PIs: Rathi, O'Donnell).

Tomasz Pieciak acknowledges the Polish National Agency for Academic Exchange for grant PPN/BEK/2019/1/00421 under the Bekker programme and the Ministry of Science and Higher Education (Poland) under the scholarship for outstanding young scientists (692/STYP/13/2018). Tomasz Pieciak, Antonio Tristán Vega and Santiago Aja-Fernández were supported by research grants PID2021-124407NBI00, funded by MCIN/AEI/10.13039/501100011033/FEDER, UE, and TED2021-130758B-I00, funded by MCIN/AEI/10.13039/501100011033 and the European Union “NextGenerationEU/PRTR”. Dominika Ciupek, Maciej Malawski and Julia Machnio were supported by the European Union’s Horizon 2020 research and innovation program under grant agreement Sano No 857533 and the International Research Agendas program of the Foundation for Polish Science No MAB PLUS/2019/13.

JYMY and SG received positional funding from the Royal Children’s Hospital Foundation (RCHF 2022-1402). CEK was supported by an Australian Government Research Training Program (RTP) Scholarship, Monash University (Monash Graduate Excellence Scholarship), and the Australian National Health and Medical Research Council (NHMRC; Centre of Research Excellence in Newborn Medicine 1153176). JYMY, SG, and CEK acknowledge the support of the Royal Children’s Hospital, Murdoch Children’s Research Institute, The University of Melbourne Department of Paediatrics, and the Victorian Government’s Operational Infrastructure Support Program. Ye Wu was supported by the National Natural Science Foundation of China (No. 62201265). The content is solely the responsibility of the authors and does not necessarily represent the official views of the NIH.

## References

1. Aganj, I., Lenglet, C., Sapiro, G.: Odf reconstruction in q-ball imaging with solid angle consideration. In: Proceedings/IEEE International Symposium on Biomedical Imaging: From Nano to Macro. IEEE International Symposium on Biomedical Imaging 2009, vol. 1398 (2009). <https://doi.org/10.1109/ISBI.2009.5193327>
2. Annett, M.: A classification of hand preference by association analysis. *Brit. J. Psychol.* **61**, 303–321 (1970). <https://doi.org/10.1111/J.2044-8295.1970.TB01248.X>
3. Cetin-Karayumak, S., Zhang, F., O'Donnell, L.J., Rathi, Y.: Harmonization of multi-site diffusion magnetic resonance imaging data from the adolescent brain cognitive development study. *Biol. Psychiat.* **91**, S84 (2022). <https://doi.org/10.1016/j.biopsych.2022.02.227>
4. Chandio, B.Q., Olivetti, E., Romero, D., Harezlak, J., Garyfallidis, E.: Bundlewarp, streamline-based nonlinear registration of white matter tracts. In: bioRxiv, pp. 2023–01 (2023)

5. Chandio, B.Q., et al.: Bundle analytics, a computational framework for investigating the shapes and profiles of brain pathways across populations (2020). <https://doi.org/10.1038/s41598-020-74054-4>
6. Fischl, F.B.: Freesurfer (2012). <https://doi.org/10.1016/j.neuroimage.2012.01.021>
7. Garyfallidis, E.: Towards an accurate brain tractography [phd thesis]. University of Cambridge, United Kingdom (2012)
8. Heinsfeld, A.S., Franco, A.R., Craddock, R.C., Buchweitz, A., Meneguzzi, F.: Identification of autism spectrum disorder using deep learning and the abide dataset. *NeuroImage: Clin.* **17**, 16 (2018). <https://doi.org/10.1016/J.NICL.2017.08.017>
9. Jernigan, T.L., et al.: The pediatric imaging, neurocognition, and genetics (ping) data repository. *NeuroImage* **124**, 1149 (2016). <https://doi.org/10.1016/J.NEUROIMAGE.2015.04.057>
10. Koo, T.K., Li, M.Y.: A guideline of selecting and reporting intraclass correlation coefficients for reliability research. *J. Chiropractic Med.* **15**, 155–163 (2016). <https://doi.org/10.1016/J.JCM.2016.02.012>
11. Magnotta, V.A., et al.: Multicenter reliability of diffusion tensor imaging. *Brain Connect.* **2**, 345 (2012). <https://doi.org/10.1089/BRAIN.2012.0112>
12. Marcus, D.S., Wang, T.H., Parker, J., Csernansky, J.G., Morris, J.C., Buckner, R.L.: Open access series of imaging studies (oasis): cross-sectional MRI data in young, middle aged, nondemented, and demented older adults. *J. Cogn. Neurosci.* **19**, 1498–1507 (2007). <https://doi.org/10.1162/JOCN.2007.19.9.1498>
13. Ning, L., et al.: Multi-shell diffusion mri harmonisation and enhancement challenge (mushac): Progress and results. In: *Mathematics and Visualization*, pp. 217–224 (2019). [https://doi.org/10.1007/978-3-030-05831-9\\_18/COVER](https://doi.org/10.1007/978-3-030-05831-9_18/COVER)
14. Petersen, R.C., et al.: Alzheimer’s disease neuroimaging initiative (adni): clinical characterization. *Neurology* **74**, 201 (2010). <https://doi.org/10.1212/WNL.0B013E3181CB3E25>
15. Pizzolato, M., Palombo, M., Hutter, J., Nash, V., Zhang, F., Gyori, N.: Super-resolution of multi dimensional diffusion mri data (2020). <https://doi.org/10.5281/ZENODO.3718990>
16. Rubinov, M., Sporns, O.: Complex network measures of brain connectivity: uses and interpretations. *NeuroImage* **52**, 1059–1069 (2010). <https://doi.org/10.1016/J.NEUROIMAGE.2009.10.003>
17. Schilling, K.G., et al.: Fiber tractography bundle segmentation depends on scanner effects, vendor effects, acquisition resolution, diffusion sampling scheme, diffusion sensitization, and bundle segmentation workflow. *NeuroImage* **242**, 118451 (2021). <https://doi.org/10.1016/J.NEUROIMAGE.2021.118451>
18. Somerville, L.H., et al.: The lifespan human connectome project in development: a large-scale study of brain connectivity development in 5–21 year olds. *NeuroImage* **183**, 456 (2018). <https://doi.org/10.1016/J.NEUROIMAGE.2018.08.050>
19. Strike, L.T., et al.: queensland twin imaging (qtim) (2023). <https://doi.org/10.18112/openneuro.ds004169.v1.0.7>
20. Tax, C.M., et al.: Cross-scanner and cross-protocol diffusion mri data harmonisation: a benchmark database and evaluation of algorithms. *NeuroImage* **195**, 285–299 (2019). <https://doi.org/10.1016/j.neuroimage.2019.01.077>
21. Vollmar, C., et al.: Identical, but not the same: intra-site and inter-site reproducibility of fractional anisotropy measures on two 3.0 t scanners. *NeuroImage* **51**, 1384–1394 (2010). <https://doi.org/10.1016/J.NEUROIMAGE.2010.03.046>